Int J Adv Manuf Technol (2018) 94:4479–4491
https://doi.org/10.1007/s00170-017-1176-2

ORIGINAL ARTICLE

Failure mechanisms of refill friction stir spot welded 7075-T6 aluminium alloy single-lap joints

Andrzej Kubit[1] · **Magdalena Bucior**[1] · **Dawid Wydrzyński**[1] · **Tomasz Trzepieciński**[2] · **Maciej Pytel**[3]

Received: 25 May 2017 / Accepted: 28 September 2017 / Published online: 5 October 2017

Abstract The goal of investigations included in this paper is to determine the effect of welding parameters on the load capacity of joints and an analysis of the defects in welded single-lap joints obtained by the refill friction stir spot welding method. Furthermore, a study is made of the effect of welding parameters on the tensile strength and fracture mode of joints subjected to tensile/pure shear loading. The overlapping friction stir spot welded joints are made of two 7075-T6 aluminium alloy sheets with different thicknesses (1.6 and 0.8 mm). The evaluation of joint quality was done using optical microscopy and scanning electron microscopy. The load capacity of joints is determined in tensile/pure shear loading tests. Microstructural analysis showed that the important parameters affecting the quality of the joints are the duration of welding and tool plunge depth. Depending on the tool plunge depth, three types of joint damage were observed. The test results indicate that incorrect selection of welding process parameters results in defects such as voids, hooks, onion rings and bonding ligament.

Keywords Refill friction stir spot welding · RFSSW · Joining · 7075-T6 · Aluminium alloy

✉ Tomasz Trzepieciński
tomtrz@prz.edu.pl

[1] Department of Manufacturing and Production Engineering, Rzeszow University of Technology, 8 Powst. Warszawy Ave, 35-959 Rzeszów, Poland

[2] Department of Materials Forming and Processing, Rzeszow University of Technology, 8 Powst. Warszawy Ave, 35-959 Rzeszów, Poland

[3] Department of Materials Science, Rzeszow University of Technology, W. Pola 2 Str., 35-959 Rzeszow, Poland

1 Introduction

Refill friction stir spot welding (RFSSW) is a technology used to join material, mainly in the automotive and aerospace industries, for instance, in panel structures and load-bearing constructions. RFSSW was developed and patented by the GKSS GmbH in Germany [1]. This method consists in spot friction heating of the joint by a rotary tool. The tool is made of two parts (pin and sleeve), and the hole that results from withdrawal of the tool is filled. As a result, the spot weld has much greater strength. The refilling process improves the tensile strength of the RFSSW joint and can also be used to repair fatigue cracks. The RFSSW method is an alternative to resistance spot welding (RSW), riveting and conventional welding. The resistance spot welding of aluminium alloys is more difficult than steel because of electrical conductivity of aluminium is high, and high currents with exact pressures have to be applied to melt aluminium sheets. The problems existed in RSW of aluminium alloys, such as liquation cracking, solidfication cracking and porosity [2] can be eliminated with FSSW. The most common approach for ensuring the weld with suitable quality is the selection of appropriate welding parameters, i.e., welding current, welding time and welding force [3].

RFSSW is a variation of linear friction stir welding (FSW). FSW is a process of joining metals in the solid state. FSW is characterised by low energy consumption [4], no gas emission and no need for consumable materials such as electrodes, filler metals or shielding gases, and therefore, it is considered as a green and environmentally friendly welding technology [5]. Unfortunately, this process has a tendency to lead to the occurrence of defects that spread along the weld line. These defects are generally caused by unsuitable parameters of the welding process or improper technological conditions. Defects that occur in FSW joints differ significantly from the

defects observed for RFSSW joints or conventional welding and should be defined separately [6]. Unfortunately, there are no standards available for RFSSW technology to assess the incompatibility of joints. Available standards correspond to FSSW welding technology. In the standard EN ISO 25239-5 [7], examples of incompatibilities that may occur in welded joints are presented, whereas in AWS D17.3 [8], information on the quality levels of FSW joints can be found. Defect detection methods divide the defects into two categories, external and internal, in the process of FSW. Because defect formation in FSW is very different from that in arc welding, Gibson et al. [9] provided a classification of FSW defects. FSW defects include excessive flash, excessive concavity, tool particulate inclusions, foreign substances, voids, wormholes, lack of penetration, root defects and kissing bond defects which may occur in the root or in the weld interior. External defects can be detected using visual methods. Internal defects such as wormholes, inclusions of solid particles from tools, surface contamination, voids and incomplete penetration can occur both inside the joint and on the face of the joint surface [9]. Defects can be also divided into microscopic and macroscopic, depending on their size.

RFSSW is a new technology for joining materials. It is most frequently used for joining aluminium alloys such as 7075-T6 [10], 6061-T6 [11] and 6181-T4 [12] and AZ31 magnesium [13] alloy components.

Among the many aluminium alloys, the 7075-T6 alloy has been extensively studied with regard to FSW and RFSSW processes. The 7075-T6 is a precipitation-hardened Al–Zn–Mg–(Cu) alloy that has been extensively used for high load constructional elements in aircraft structural components. This material is a kind of non-weldable material and is characterised by low resistance to oxidation. Furthermore, the 7075-T6 alloy has a high mechanical strength comparable with that of structural steel and a very high fatigue resistance, has an average resistance to corrosion and is very well suited for grinding, polishing and spark erosion.

Nowadays, spot welding is replacing riveting and adhesive bonding of light metal alloys due to their numerous advantages, such as the following:

- drilling of joined components is not required;
- the use of rivets as additional joining elements is not required;
- the load capacity of welds can reach values higher than that of riveted joints;
- welded joints preserve high corrosion resistance due to the absence of additional elements with other electrochemical potential;
- parts of the weld do not protrude above the surface of joined elements;
- there is the possibility of a simple repair of the joint;
- the possibility of leakage through the joint is eliminated.

However, the state of knowledge of the phenomena occurring during the welding process is not complete, which results in difficulties in the selection of the optimum process conditions for the particular alloys used in the aerospace industry. Although, many publications describe the RFSSW technology, many welding problems remain unresolved. The problem with ensuring high quality joints is also connected with a lack of standards for RFSSW.

Shen et al. [10] investigated the mechanical properties of 7075-T6 aluminium alloy joints joined by the RFSSW process. The joint strength is investigated in terms of hardness and tensile/shear and cross-tension test. They found that the void in the weld played an important role in determining the strength of the joint as well as the main feature affecting the mechanical properties of the joint is the connecting qualities between the stir zone and the thermo-mechanically affected zone. Furthermore, the alclad between the upper and the lower sheets lowered the joint strength. Zhang et al. [14] studied the effect of the rotational speed and dwell time on the mechanical properties and microstructure of normal and walking FSSW joint of 5052-H12 aluminium alloy sheets. The results indicate that the joint strength decreases with increasing rotational speed, while it is not affected significantly by dwell time. It was found that performance of the welds plays a predominant role in determining the tpye of fracture mode. The effects of the processing conditions on the strengths and failure modes of two types of dissimilar friction spot welds between aluminium alloy 5754-O and 7075-T6 sheets are investigated by Tran et al. [15]. The experimental results indicate that the failure loads of both types of welds 5754/7075 and 7075/5754 in lap–shear specimens increase when the processing time increases for the given ranges of the processing time. The optical micrographs show and different failure modes and different weld geometries of the welds made at different processing times. Merzoug et al. [16] conducted the experiments of friction spot stir welding to assess the effects of welding feed rate and tool rotating speed on FSW process of 6060-T5 aluminium alloys. They conclude that the quality of the welded joint is all the more important, as the tool rotating speed is decreased and that welding feed rate is increased. The results of investigations of joining AA6181-T4 aluminium alloy conducted by Rosendo et al. [12] revealed that sound connections can be produced.

Shen et al. [10] investigated the mechanical properties of 7075-T6 aluminium alloy joints joined by the RFSSW process. The joint strength is investigated in terms of hardness and the tensile/shear and cross-tension test. They found that the void in the weld played an important role in determining the strength of the joint as well as finding that the main feature affecting the mechanical properties of the joint is the quality of the connection between the stir zone and the thermo-mechanically affected zone. Furthermore, the alclad between the upper and the lower sheets reduced the joint strength.

Zhang et al. [14] studied the effect of the rotational speed and dwell time on the mechanical properties and microstructure of normal and walking FSSW joints in 5052-H12 aluminium alloy sheets. The results indicate that the joint strength decreases with increasing rotational speed, while it is not significantly affected by dwell time. It was found that the performance of the welds plays a predominant role in determining the type of fracture mode. The effects of the processing conditions on the strengths and failure modes of two dissimilar types of friction spot welds between aluminium alloy 5754-O and 7075-T6 sheets are investigated by Tran et al. [15]. The experimental results indicate that the failure loads of both types of welds 5754/7075 and 7075/5754 in lap–shear specimens increase when the processing time increases for the given ranges of processing time. The optical micrographs show different failure modes and different weld geometries of the welds made with different processing times. Merzoug et al. [16] conducted the experiments of friction spot stir welding to assess the effects of welding feed rate and tool rotation speed on the FSW processing of 6060-T5 aluminium alloys. They conclude that the quality of the welded joint is all the more important, as the tool rotation speed is decreased and welding feed rate is increased. The results of investigations of joining AA6181-T4 aluminium alloy conducted by Rosendo et al. [12] revealed that sound connections can be produced; high strength connections were associated with joining times between 2.6 and 3 s, particularly when coupled with low rotation speeds (1900 rpm). The examination of the macro-/microstructural cross-sections revealed the presence of three important geometric and metallurgical features: partial bonding, bonding ligament and hooking. Choi et al. [17] investigated the joint strength of friction stir spot welded 5J32 Al alloy according to the three tool penetration depths (threaded pin tool, cylindrical tool and cylindrical tool with projection) and tool shape. They found that in the case of a cylindrical tool with projection, the tensile shear load rapidly increased with increasing tool penetration depth. For a cylindrical tool and threaded pin tool, the vertical joint deformation increased with tool penetration depth, whereas the tensile shear load did not increase. In the work of Xu et al. [18], the RFSSW was used to weld 2-mm-thick 5083-O aluminium alloy according to the Box–Behnken experimental design which was used to study the effect of welding parameters on the joint lap–shear strength and joint properties. It was found that the stir zone was higher than that of the base material and the hardness decreased with increasing the heat input during welding. The fracture modes obtained during the lap–shear test were affected by the hook defect.

Zhao et al. [19] investigated material flow behaviour and temperature during FSSW of Alclad 7B04-T74 aluminium alloy both by experiment and by numerical simulation. The peak temperatures in the thermo-mechanically affected zone and the heat-affected zone were lower than the solution temperature and higher than the artificial ageing temperature of the base material. The authors also reported that a thick bonding ligament at the base material surfaces at the joint centre was composed of the original alclad layers. Li et al. [20] investigated the RFSSW of 2024-T4 aluminium alloy to find the effects of welding parameters on the fracture modes of tensile–shear loaded joints. It was reported that fracture modes are largely influenced by sleeve plunge depth and are mainly determined by the bonding strengths of the lap interface and the stir zone/thermo-mechanically affected zone interface. Cao et al. [21] investigated the texture, evolution of the microstructure and mechanical properties during the RFSSW of the 6061-T6 aluminium alloy. They concluded that the microstructure evolution was governed by grain subdivision and geometric dynamic recrystallisation, but also involving limited static recrystallisation. It was also concluded that the hook height had a negative effect on tensile shear strength. Zhao et al. [22] experimentally investigated the FSW process of 7B04-T74 aluminium alloy sheets and the effects of sleeve plunge depth on mechanical properties and weld appearance. The authors noticed that a deep plunge depth tended to make the alclad more dispersed in the weld, creating a satisfactory joint. However, if the plunge depth is too deep, the excessive bending of the hook can unfavourably affect the strength of the joint. Reimann et al. [23] presented a solution for closing termination holes or flaw repairs using RFSSW by using semi-stationary shoulder bobbin tool. The results of welding of 2198-T851 aluminium alloy sheets show defect free and highly efficient joints. The mechanical performance of keyhole closure welds using the method developed was comparable to the performance of keyhole closure welds in bare sheets. Reimann et al. [24] investigated the evolution of microstructural features and the mechanical strength of RFSSW joints of 7075-T651 aluminium alloy sheets. They found that the dwell time decreases the weld strength, as yield stress is reduced by 10% when 6 s of dwell time are applied during RFSSW. The high plunge depth caused partial recrystallisation in the centre of the weld.

This paper focuses on an analysis of the defects arising during the RFSSW welding process. The effect of various process parameters on the quality and strength properties of the single-lap joints is also analysed. The quality of joints is evaluated using optical microscopy, scanning electron microscopy and the results of tensile/pure shear tests of the joints.

2 Materials and methods

The experimental investigations of the RFSSW process of 7074-T6 aluminium alloy sheets were conducted using an RPS100 spot welder by Harms & Wende GmbH & Co KG (Hamburg, Germany). Due to its high strength properties and

Table 1 Chemical composition of the 7075-T6 aluminium alloy (wt%)

Si	Fe	Cu	Mn	Mg	Cr	Zn	Ti	Other impurities		Al
								Single	Total	
0.40	0.50	1.2 ÷ 2.0	0.30	2.1 ÷ 2.9	0.18 ÷ 0.35	5.1 ÷ 6.1	0.20	0.05	0.15	Rest

good corrosion resistance, the 7075-T6 aluminium alloy is commonly used in the aerospace industry [10]. The chemical composition and basic mechanical properties of the joined sheet material are presented in Tables 1 and 2, respectively. In the joining of aerospace structures, the RFSSW technique can be used as an alternative to resistance welding. An example of its application may be, for example, welding of a skin plate of an aircraft with a stiffening stringer. As a result, two different thicknesses of 1.6 and 0.8 mm were selected for the welding investigations (Fig. 1a). To ensure repeatability of the connections, the samples were welded in a special instrument (Fig. 1b).

The welding process was carried out for different values of welding parameters, that is, tool rotational speed, duration of welding and tool plunge depth. The spindle speed n was varied in the range of 2000–2800 rpm, the duration of welding t in the range of 1.5–3.5 s and the tool plunge depth g in the range of 1.5–1.9 mm. Research began at the highest rotational speed and the middle value of plunge depth and plunging time. Such joints were subjected to microstructure analysis and strength tests, and on the basis of this analysis, it was decided to select parameters for the next step. The analysis of joint quality and the selection of new parameters were repeated several times as shown in the block scheme (Fig. 2).

The strength tests were performed on a Zwick/Roell Z100 tensile machine. Welded samples were subjected to static tensile/pure shear loading. To ensure pure shear loading (Fig. 3a), the specimens were fixed in a special holder (Fig. 3b). The crosshead travel speed in the case of the tensile/shear loading was set to 5 mm/min.

Microstructural examination of the RFSSW samples was carried out using a Nikon Epiphot 300 light microscope with the NIS Elements V2.3 software as well as a Hitachi S3400N scanning electron microscope equipped with a Thermo Scientific Ultra Dry EDS Detector and Thermo Scientific™ NORAN™ System 7 for microanalysis of the chemical composition using an energy-dispersive X-ray spectroscopy technique. Macroscopic examination was also conducted using an Opta-Tech X2000 stereoscopic microscope. Metallographic specimens were prepared according to ASTM E407 [25] by the following procedure: the samples were first cut using a Struers Accutom-50 precision machine and then mounted in Struers Polyfast resin using a Struers LaboPress-3. The microsections were prepared in accordance with the following procedure: grinding with abrasive papers down to 1200 grit size and polishing using diamond suspensions (9, 6, 3 and 1 μm). Microsections were etched with Keller's reagent, which had a composition of 2 ml of HF, 3 ml of HCL and 5 ml of HNO_3 diluted in 190 ml of distilled water, and the etching time was about 10 s.

3 Results

3.1 Microstructural observations

The macroscopic and microscopic observations of the cross-section of the weld made at different welding conditions of rotational speed, welding time and sleeve plunge depth are presented in Figs. 4, 5, 6, 7, 8, 9, 10, 11, 12 and 13. The cross-section of the RFSSW joints (Figs. 4, 5 and 6 and 8, 9 and 10) can be divided into four regions in terms of the microstructural characteristics of the joint in sequence from the stir zone (SZ) towards the base material (BM) [10]: the SZ, the thermo-mechanically affected zone (TMAZ), the heat-affected zone (HAZ) and the BM. In the SZ, a homogenous fine-grained microstructure was found, which was characterised by fully dynamically recrystallised equiaxial grains with an average diameter of about 5 μm, as shown in Fig. 12a. This effect probably occurs due to a lack of mixing of the alloy, poor formability of materials and inappropriate processing parameters.

The presence of the HAZ was also observed, but it was not seen in all cross-sections. In the HAZ, the grains are similar to those of the BM, but in the direction of the TMAZ, the grains

Table 2 Mechanical properties of the 7075-T6 aluminium alloy

As received	Tensile stress R_m (MPa)	Yield stress $R_{p0.2}$ (MPa)	Elongation A (%)
T6	482.6	413.68	7

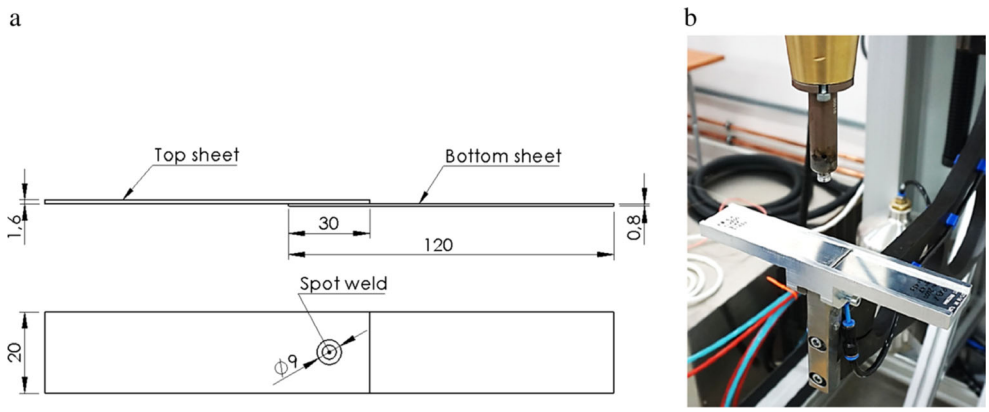

Fig. 1 **a** The shape and dimensions of the welding specimens. **b** The attachment for positioning the specimens

become slightly coarse (Fig. 4). On the boundary between HAZ and TMAZ, the grains begin to deform (Figs. 9a and 10). Figures 8a, b, 9b and 10 show the direction of the material flow in the TMAZ.

In the structure of the joints made at the tool speed of 2000 rpm, a clear structural notch (Fig. 6a, b) and distinct structural discontinuities in the weld nugget are visible and may be a source of fatigue notches.

In the cross-sectional area of the joint, we can see the clear area of the bonding ligament in the middle part of the joint (Figs. 7 and 8b), which, due to the elevated temperature of the joint, penetrates the weld area, which may lower the strength of the joint.

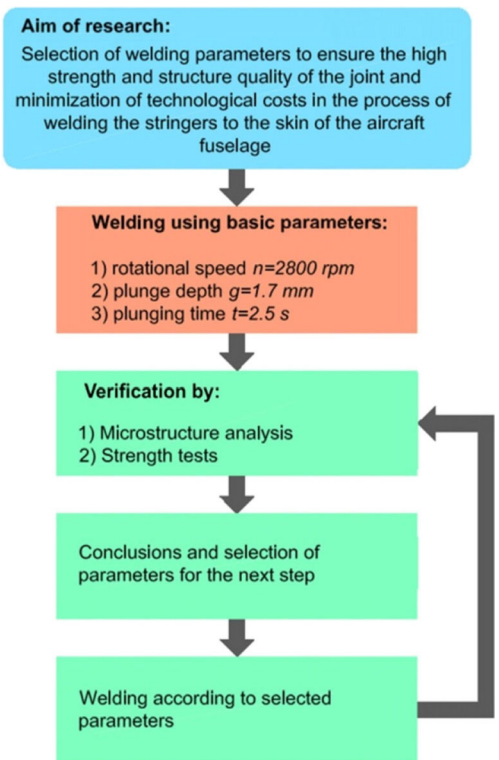

Fig. 2 Block scheme of the selection process of welding parameters

In general, within the centre of the SZ in the RFSSW process, a fine-grained microstructure is observed (Fig. 9a). In the case of the TMAZ, a high gradient of grain size change is revealed (Fig. 9b). A subgrained microstructure was found, as shown in Figs. 10 and 12b. On the boundary of these grains, ultrafine precipitates were observed. Literature data suggest that these are probably particles of Al_7Cu_2Fe, Mg (Zn, Cu, Al)$_2$ and also $MgZn_2$ strengthening phases that occur in the 7xxx series aluminium alloys [26].

At a tool rotational speed of $n = 2000$ rpm, $g = 1.5$ mm and $t = 3.5$ s, a visible subgrained microstructure is observed within the microarea between the TMAZ and the HAZ (Fig. 10). An increase in the tool rotational speed to 2400 rpm and a decrease of the duration of welding to 1.5 s lead to the observation of grains that are elongated in the rolling direction on the side of the BM (Fig. 11a). Furthermore, within the SZ of the joint, a dynamically recrystallised fine-grained structure with equiaxial grains is observed (Fig. 11b). Further increase of the values of all controlled welding parameters causes an increase of the dynamically recrystallised fine-grained microstructure with equiaxial grains within the centre of the SZ (Fig. 12a). On the other hand, within the area between the

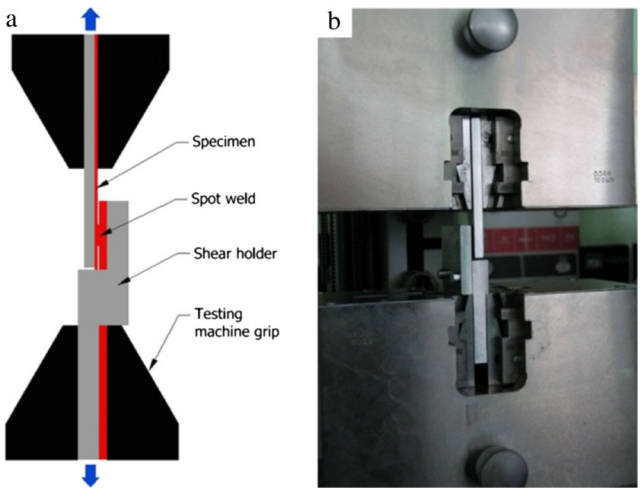

Fig. 3 Scheme of fixing the specimen for the tensile/shear test (**a**) and view of real test fixture (**b**)

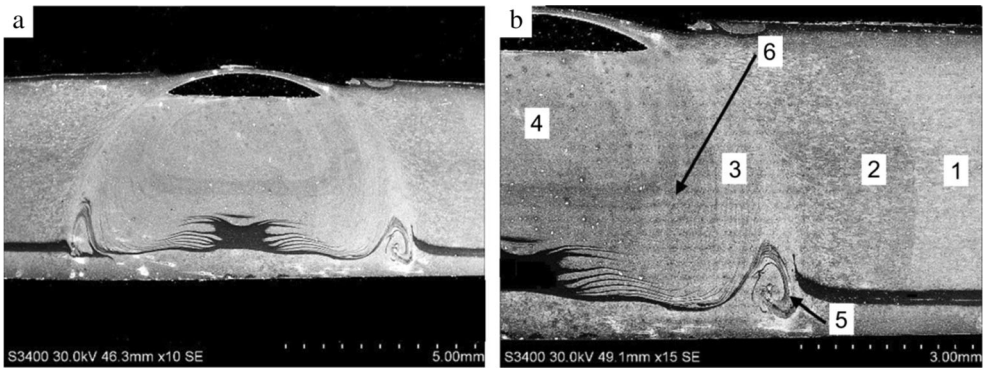

Fig. 4 SEM macrostructure of RFSSW joint of 7075 aluminium alloy sheets (n = 2800 rpm; g = 1.7 mm; t = 2.5 s). **a** Cross-section and **b** magnification of characteristic zones: 1 BM, 2 HAZ, 3 TMAZ, 4 SZ, 5 hook area, 6 onion rings

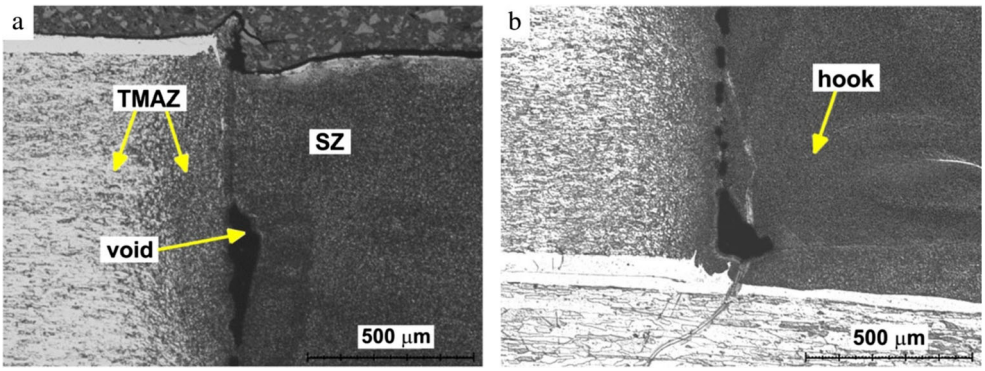

Fig. 5 Microstructure of RFSSW joint of 7075 aluminium alloy (n = 2600 rev/min; g = 1.7 mm; t = 1.5 s). **a** Cross-section of hook area and **b** void in the hook area between SZ and TMAZ due to an incomplete refill

HAZ and the TMAZ, a subgrained microstructure can be observed (Fig. 12b).

The welding time is also an important parameter that affects the weld quality. For the time t = 1.5 s, there is a clear boundary between the welded sheet and the alclad layer (Fig. 13) separating the joined sheets, which form a thermal barrier that releases heat away from the weld area.

Within the SZ (1 in Fig. 13a, b), the visible flow of the alclad coating (2 in Fig. 13a, b) is observed. However, at the bottom-centre of the SZ, partially undeformed grains can be seen. On the basis of macro- and microstructural examinations, it was found that the microstructure of the BM in the longitudinal section of the joint was characterised by deformation texture with grains that were elongated and oriented in the rolling direction (Fig. 11).

The weld nugget has a fine-grained structure (Fig. 14a, b). In the lower zone of joint exists also an alclad layer which, although much higher temperature is not degraded. The alclad in the RFSSW joint is a specific collector that removes heat and possesses a structural notch, lowering the static strength of the joint. The increasing of welding time causes heat diffusion in the upper area of the lower sheet (Fig. 14c).

3.2 Joint strength

The strength of the joints was tested experimentally under static tensile/shear loading. Depending on the tool plunge depth, three types of joint damage were observed (Fig. 15): shear fracture (type I), plug–shear fracture (type II) and plug fracture (type III). Generally, the tensile/shear loading is the

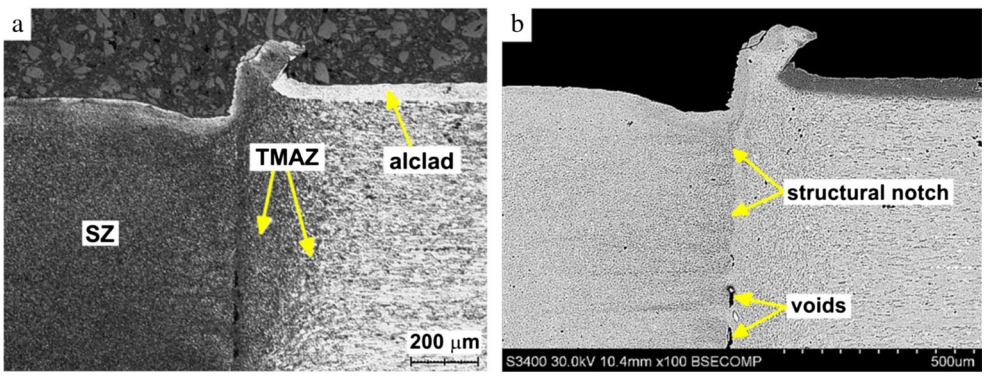

Fig. 6 Microstructure of 7075 aluminium alloy sheets with RFSSW joint (n = 2000 rpm; g = 1.5 mm; t = 3.5 s) within the area between the SZ and the TMAZ prepared using **a** optical microscopy and **b** scanning electron microscopy

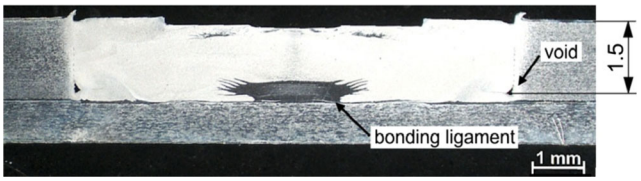

Fig. 7 Cross-sections of RFSSW joints welded at n = 2400 rpm; g = 1.5 mm; t = 1.5 s

lowest when the fracture mode is a plug-type fracture and the highest when the fracture mode is a plug–shear fracture. Furthermore, plug–shear fracture is the most preferable fracture mode under tensile/shear loading [27]. Table 3 presents the results of strength tests on the study joints.

One of the important parameters affecting the mode of damage is the tool plunge depth. For most of the joints considered, the dependence of tool plunge depth and degree of weakening of the lower sheet has been demonstrated, which is revealed in the characteristic types of failure. For the smallest tool plunge depth, g = 1.5 mm (Fig. 16a), the weld is sheared without breaking the BM. For the joint prepared at g = 1.7 mm (Fig. 16b), the plug–shear-type fracture was observed. In the case of the type III destruction, for g = 1.9 mm, there was a partial tearing of the material together with the weld nugget from the lower sheet (Fig. 16c).

The experiments indicate a great impact of tool plunge depth on the load capacity of the joint. This is also confirmed by the value of the correlation coefficient R^2, which is 0.97 in this case. For comparison, the load capacity of the joints in which the shear-type fracture was observed for the variant where g = 1.5 mm was 7.07 kN, and for n = 1.9 mm, the load capacity was 6.74 kN.

With an increase of tool plunge depth, the load capacity of the joint decreases. There is also a correlation between the duration of welding and the load capacity of the joint

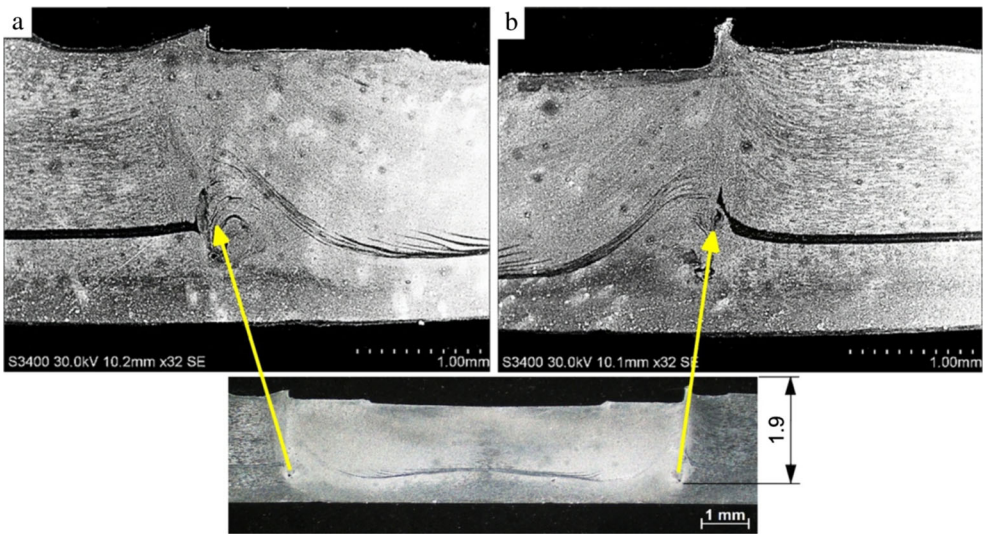

Fig. 8 Macrostructure of RFSSW joint of 7075-T6 alloy aluminium sheets (n = 2400 rpm, g = 1.9 mm, t = 3.5 s); both (**a**) and (**b**) show the microstructure within the area between the HAZ and the TMAZ zones, respectively

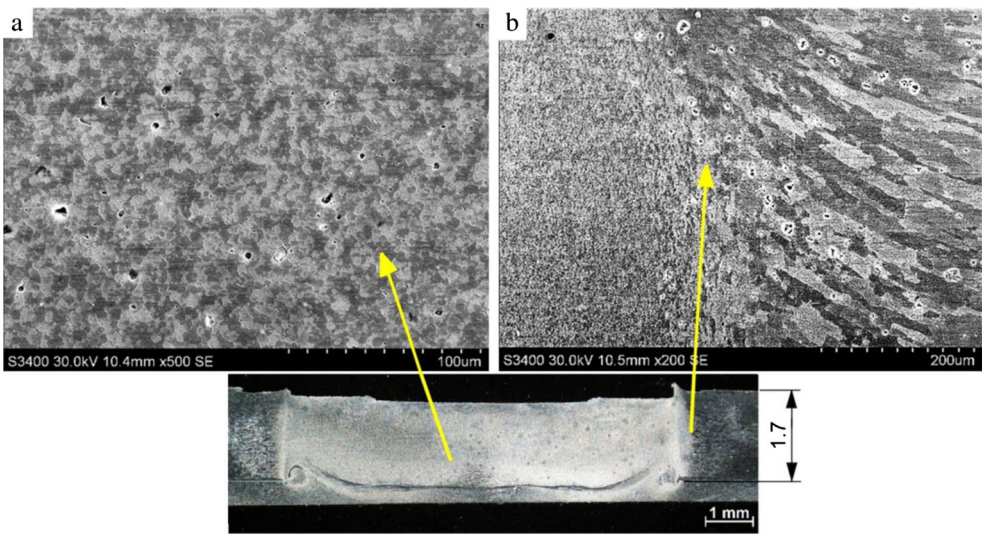

Fig. 9 Macrostructure of 7075 aluminium alloy RFSSW joint (n = 2000 rpm; g = 1.7 mm; t = 2.5 s). **a** The centre of the SZ. **b** TMAZ

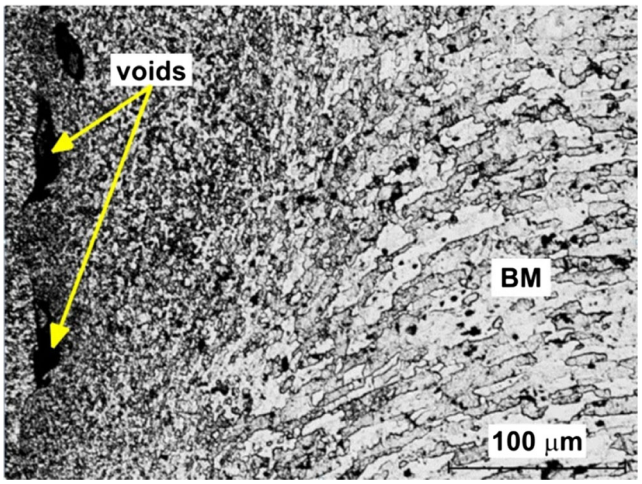

Fig. 10 Microstructure of 7075-T6 aluminium alloy RFSSW joints (n = 2000 rpm, g = 1.5 mm, t = 2.5 s)

(R^2 = 0.96). An increase in the duration of welding leads to a decrease in the load capacity of the joint. However, for a welding duration of t = 2.5–3.5, the area of tool penetration goes smoothly into the TMAZ (Figs. 7a and 8a), where there is no visible boundary between the SZ and the BM.

In general, research has shown that the most favourable plunge depth is g = 1.5 mm because in most cases the joint was destroyed in the interface plane without breaking the BM structure, and also the highest values of load capacity were obtained at this plunge depth. The results of the strength test for the plunge depth g = 1.5 mm and its dependence on rotational speed and plunging time are presented in Fig. 17.

It should be noted that with the parameters at which the highest load capacity of the joint has been obtained, i.e., n = 2400 rpm, g = 1.5 mm and t = 3.5 s, the structure of the lower sheet has been weakened leading to its failure in the form shown in Fig. 18. Such a type of damage is due to the overheating of the lower sheet, which is undesirable because it leads to weakening of the material and as a result to it being damaged at a stress much lower than its nominal tensile strength.

4 Discussion

4.1 Microstructural observations

The macroscopic and microscopic observations show that the TMAZ is concentrated in a narrow zone around the periphery of the sleeve, which experiences both moderate frictional heating and deformation and is characterised by a highly deformed structure [10]. In the TMAZ zone, recrystallization does not occur [28]. The HAZ experiences a welding thermal cycle but does not undergo plastic deformation, which causes dissolution of precipitate in the matrix [29]. As was also found by Shen et al. [10], the SZ displays a basin shape and exhibits a recrystallised and fine equiaxed grain structure due to intense plastic deformation and frictional heating during the joining process. The material is more severely stirred in the SZ than in other regions. Shen et al. [10] also observed variations in the grain sizes in the direction of thickness. This can be explained by higher temperature and severe plastic deformation under the pin and sleeve tips in the maintenance stage [10].

A clear structural notch and distinct structural discontinuities in the weld nugget are revealed in the structure of the joints and may be a source of fatigue notches. Increasing the rotational speed causes an increase in the temperature around the weld, which leads to a slight increase in the volume of the HAZ. However, in the upper part of the joint, where the rotating tool is positioned (leading to a long duration of tool interaction without penetration of the material), the structural notch is not visible. The fine-grained microstructure of the weld nugget is smoothly transformed in the HAZ. This indicates that there is a possibility that the structural notch, which lowers the load capacity of the joint, can be eliminated by modifying the setup parameters of the process.

A bonding ligament is observed in the cross-sectional area of the joint, a result of the elevated temperature of the joint, and this penetrates the weld area, which may lower the strength of the joint. The bonding ligament is higher in the centre than in the periphery of the joint, which was also

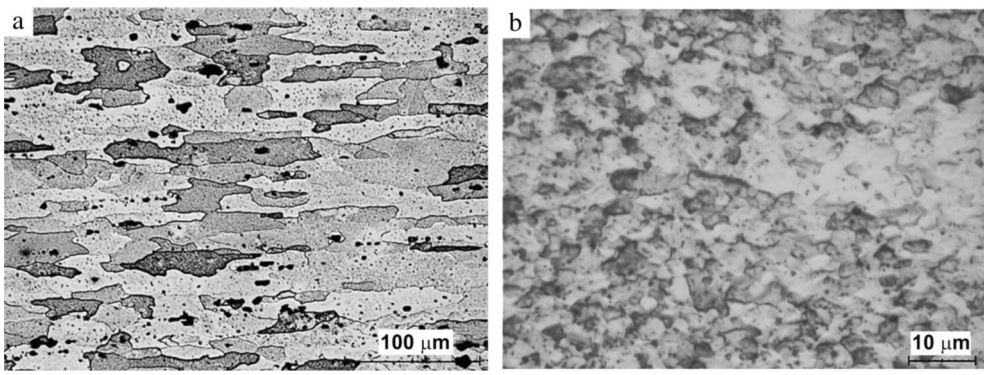

Fig. 11 A comparison of the microstructures of 7075-T6 aluminium alloy RFSSW joints (n = 2400 rpm, g = 1.5 mm, t = 1.5 s). **a** On the side of the BM. **b** Within the SZ of the sample

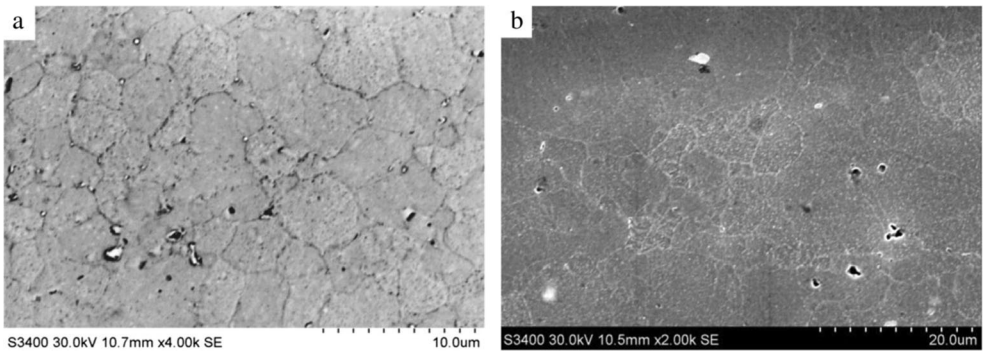

Fig. 12 Microstructure of 7075 aluminium alloy RFSSW joints (n = 2800 rpm, g = 1.7 mm, t = 2.5 s). **a** Within the centre of the SZ. **b** Within the area between the HAZ and the TMAZ

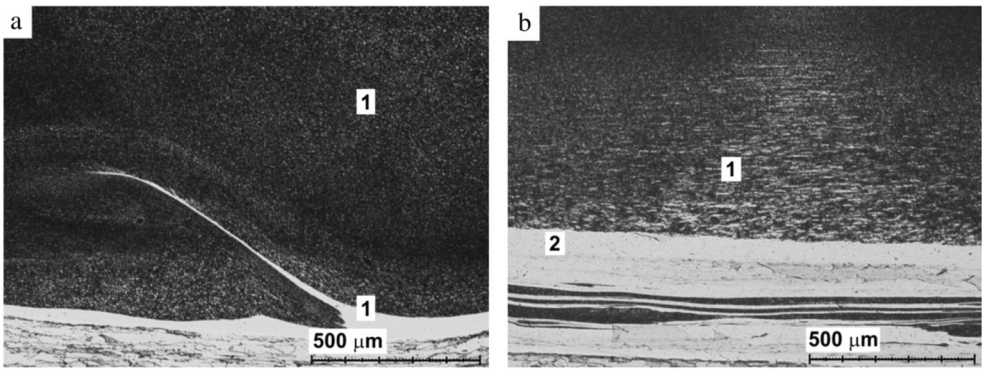

Fig. 13 Microstructure of 7075-T6 aluminium alloy RFSSW joints (n = 2600 rpm, g = 1.7 mm, t = 1.5 s). **a** At the vicinity of the joint edge. **b** At the bottom of the joint

observed by Shen et al. [10]. Ligament is formed in the pin's plunging stage, and the material in the sleeve's periphery is stirred more severely than that in the centre of the tool. It was confirmed that the macrostructure of the RFSSW joint of 7075 alloy aluminium sheets shows that ligament at the periphery of the joint (within the area between HAZ and TMAZ) is stirred with BM and the SZ is visible as an onion ring (Fig. 8b, c).

As reported by Baek et al. [30], it is expected that alclad will be stirred outwards to the edge of the spot weld in the conventional friction stir spot welding process. During the sleeve plunging process in RFSSW, the zinc coating not only moves to the edge of the spot weld but can also be partly extruded into the centre space. The layer of alclad penetrates the microstructure of the weld, which may lower its strength.

The increase in welding time clearly leads to an increase in the temperature within the weld nugget and heat diffusion in each direction. This is confirmed by an enlarged HAZ on the lateral edge of the joint and fuller reconstruction of the material structure in the location of tool plunging. Heat diffusion also occurs in the bottom area of the weld, leading to adhesive joining of the sheets. The visible HAZ, however, has a smaller width. This is due to the presence of the alclad, which has a higher thermal conductivity and transfers the heat out of the joint very quickly. The alclad layer also exists in the lower zone of the joint which, although reaching a much higher temperature, is not degraded. This process leading to adhesive joint of the sheets and reduction of grain size in lower sheet. Visible heat-affected zone, however, has a smaller width and depth. This is due to the presence of the alclad, which has a higher thermal conductivity (229 W/mK) than base material (134 W/mK) and transfers very quickly the heat out of the joint. Although RFSSW enlarges the bearing area of the spot weld, it does not lead to significant improvement in the tensile shear strength of the joint compared with conventional FSSW [31].

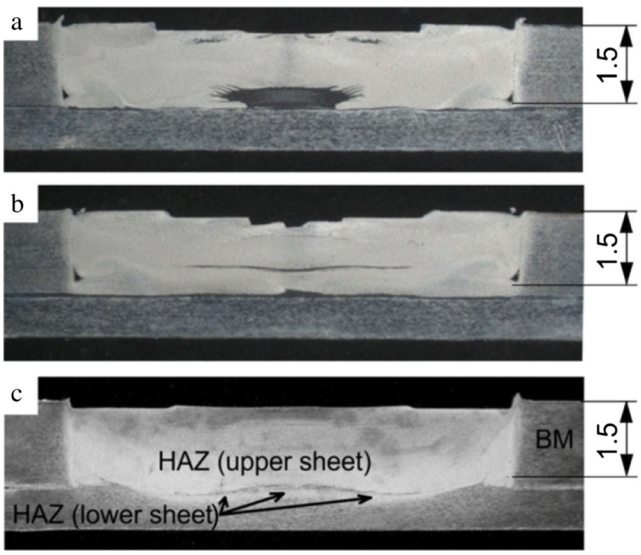

Fig. 14 Longitudinal section of RFSSW joint made under the welding conditions of a rotational speed of n = 2600 rpm, tool plunge depth of g = 1.5 mm and welding durations t of **a** 1.5 s, **b** 2 s and **c** 2.5 s

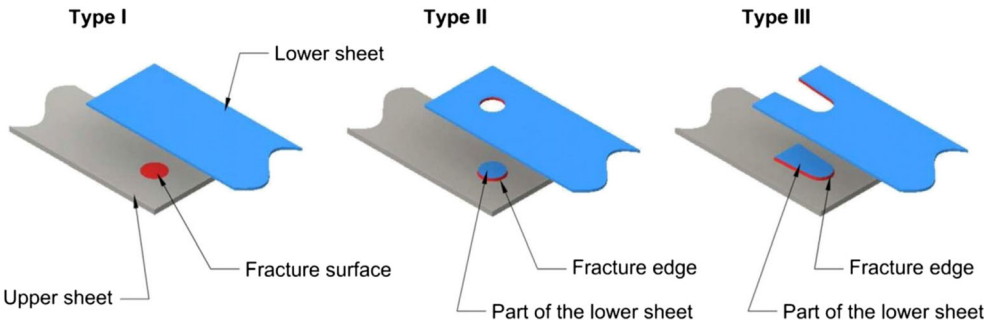

Fig. 15 Diagrams of the modes of failure observed in the shear test and its particular dependence on the plunge depth

4.2 Joint strength

The results of the strength analysis of the joints revealed that one of the important parameters affecting the mode of damage is tool plunge depth. The dependence of tool plunge depth and degree of weakening of the lower sheet have been demonstrated in most of the joints considered, which is revealed in the characteristic types of failure. For the smallest tool plunge depth, a shear fracture of the weld is observed. Shear fracture is caused by a small share of normal stresses and a high share of stress in the direction of loading. The increase in the tool plunge depth is characterised by a gradual increase in the normal stresses, which, at a tool plunge depth of 1.45 mm or above, causes a decrease in the load capacity of the joint.

Plug–shear fracture observed in the case of joints fabricated at tool plunge depth of $g = 1.7$ mm is caused by the pull-out of the nugget from the lower sheet with a blunt wedge pattern. The upper sheet has bent upward, and there is no obvious deformation of the lower sheet when the joint is subjected to loading [32]. The crack propagates inside the nugget from the bottom of the weld to the interface between the two joined sheets.

The strength tests indicate a great impact of tool plunge depth on the load capacity of the joint. Increases in tool plunge depth lead to a decrease of the load capacity of the joint. The microstructural analysis of the 7075-T6 aluminium alloy joints shows that a duration of welding that is too short contributes to incorrect phase conversion, which in turn causes defects.

The effect of tool plunge depth on the tensile shear fracture load is in agreement with the variation tendency of the fracture loads in RFSSW joints, observed by Yang et al. [33]. Rosendo et al. [12] concluded that a high rotational speed will impair the mechanical properties of RFSSW joints. Some researchers reported that plunge depth is the most important parameter influencing the joint strength [34].

Experimental tests have shown that the most favourable plunge depth is $g = 1.5$ mm, because in most cases, the joint was destroyed in the interface plane without breaking the base material structure, and also, the highest values of load capacity were obtained at this plunge depth. Rotational speed and plunging time are closely related parameters. Both increases lead to an increase in the heat range of the welded materials as a result of frictional forces, which, when exceeded by a certain

Table 3 Results of the strength tests

No.	Spindle speed n (rpm)	Tool plunge depth g (mm)	Duration of welding t (s)	Load capacity (N)
1	2000	1.5	1.5	6870
2	2000	1.5	2.5	6910
3	2000	1.5	3.5	7000
4	2000	1.7	2.5	6735
5	2400	1.5	1.5	7070
6	2400	1.5	2.5	7020
7	2400	1.5	3.5	7585
8	2400	1.9	1.5	5645
9	2400	1.9	3.5	6740
10	2600	1.5	1.5	7025
11	2600	1.5	2	6975
12	2600	1.5	2.5	6890
13	2600	1.5	3.5	7095
14	2600	1.7	1.5	6920
15	2800	1.7	2.5	6980

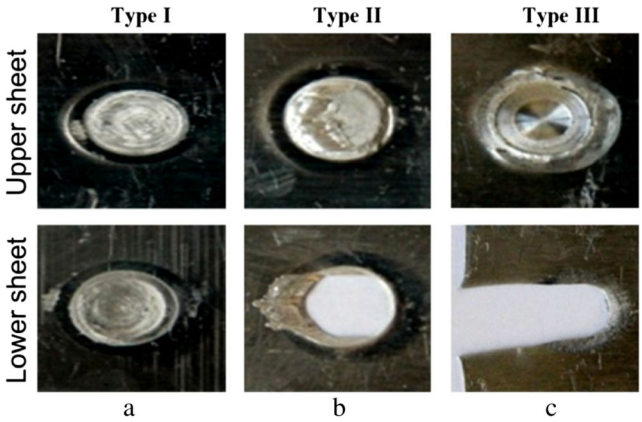

Fig. 16 Illustration of types of failure modes observed under the shearing test. **a** $n = 2400$ rpm, $g = 1.5$ mm, $t = 1.5$ s. **b** $n = 2800$ rpm, $g = 1.7$ mm, $t = 2.5$ s. **c** $n = 2400$ rpm; $g = 1.9$ mm, $t = 3.5$ s

critical value, leads to the overheating of the sheets and thus their weakening. Further studies should be carried out to further specify the influence of rotational speed and plunging time on the tool wear and then correlate these parameters with parameters that ensure high load capacity of the joint, no structural defects and damage in the interface plane.

5 Summary and conclusions

The investigations were focused on the determination of the influence of welding parameters on the load capacity of joints and the analysis of defects occurring in RFSSW joints. The experimental results allow the following conclusions to be drawn:

1. The microscope observations of the cross-section of the weld showed that in the stir zone, a homogenous fine-grained microstructure was found, which was characterised by fully dynamically recrystallised equiaxial grains with an average diameter of about 5 μm. This effect occurs due to a lack of mixing of the alloy, which was also observed by Campanelli et al. [35], who also stated that both the lack of material mixing and the pronounced vertical displacement of the hook resulting from the slipping interfacial condition established between the welding tool and the plasticised material are detrimental to the mechanical strength of the weld. Furthermore, the lack of mixing of the two sheets due to the poor flowability of materials and insufficient pressure in such a tight space, as well as the tool penetration into the bottom sheet, led to hook formation [10]. The lack of a suitable mixing of material on the faying surface is manifested in the form of a kissing bond [36]. The formation of a kissing bond can be also associated with inadequate heat and higher flow stresses.
2. Important parameters affecting the quality of the joint are the duration of welding time and tool plunge depth. However, a tool rotational speed and welding time that are too great cause overheating of the sheet material and an increase in the area of the heat-affected zone. The conclusion obtained is in agreement with the results of joining the 5042 aluminium alloy by Tier et al. [22] who suggested that sleeve plunge depth played the most important role in the tensile shear properties of the joints. The experiments indicate a great impact of tool plunge depth on the load capacity of the joint. With an increase of tool plunge depth, the load capacity of the joint decreases. The results obtained are in agreement with the results of Zafar et al. [34].
3. Increasing the rotational speed causes an increase in the temperature around the weld, which leads to a slight increase in the volume of the heat-affected zone. Yuan et al. [37] studied the effect of process parameters on the properties of the 6016 aluminium alloy FSSW joints and

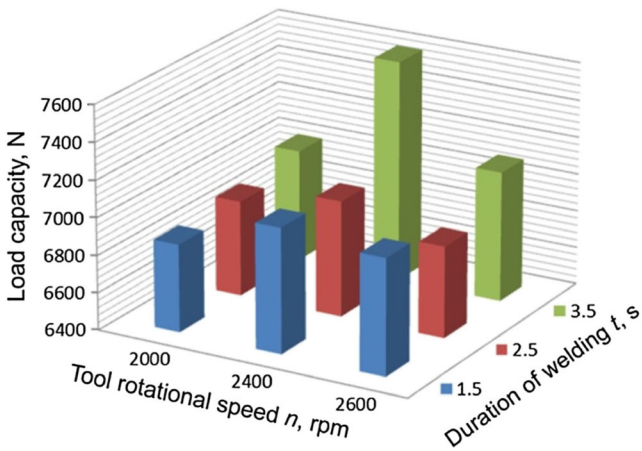

Fig. 17 Effect of tool rotational speed n and the duration of welding t on the load capacity of a joint at constant plunge depth $g = 1.5$ mm

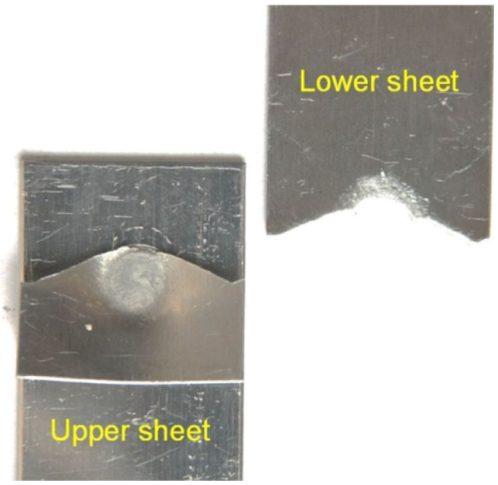

Fig. 18 Illustration of the failure mode of a joint welded according to the following parameters: $n = 2400$ rpm, $g = 1.5$ mm, $t = 3.5$ s

concluded that the tool rotational speed had most influence on lap–shear separation loads.

4. In the case of shorter welding times and a tool speed of 2000 rpm, distinct structural discontinuities are visible in the weld nugget. For longer welding times (t = 2.5–3.5 s), a lack of a structural notch was observed between the stir zone and the thermo-mechanically affected zone, which has a positive influence on the strength of the welded joints. The lack of sufficient mechanical mixing during the FSSW process can destroy the weld properties by restricting the mobility of the material around the tool pin, which is supported by the results of Pourali et al. [38].
5. The bonding ligament formed in the plunge stage of the pin in the sleeve's periphery is stirred more than that in the centre of the tool. To eliminate the bonding ligament, which decreases the weld strength, it is necessary to increase the tool rotational speed and duration of welding. The experiments conducted by Trier et al. [39] have also shown that the bonding ligament was reduced for joints produced at a higher tool rotational speed, which increases the shear strength of the joint.
6. The increase in the welding time leads to an increase in the temperature within the weld nugget and heat diffusion in each direction. The increase of welding time beneficially influencing the shear strength of the joints by good metallurgical bonding and mechanical mixing was also previously observed by Pourali et al. [38].
7. Alclad is the specific collector of heat transfer, because it has a higher thermal conductivity and very rapidly transfers the heat out of the joint. The alclad layer can reduce the strength of the bonding interface, so the tensile strength of the joint is reduced. As observed in this paper, a larger sleeve plunge depth can facilitate the downward migration of this alclad layer. Zhao et al. [22] have also concluded that this effect is beneficial for the tensile shear properties of the FSSW joints.
8. For the smallest tool plunge depth, g = 1.5 mm, the weld is sheared without breaking the base material. For the joint prepared at g = 1.7 mm, a plug–shear-type fracture was observed. In the case of g = 1.9 mm, the material together with the weld nugget was partially torn from the lower sheet indicating a plug fracture.

References

1. Schilling C, dos Santos J (2005) Verfahren und vorrichtung zum verbinden von wenigstens zwei aneinanderliegenden werkstücken nach der methode des reibrührschweißens. Germany Patent DE 19955737B4 10
2. Bayramoglu M, Esme U, Geren N (2003) Effects of welding parameters on the quality of resistance spot welded SAE 1010 steel sheet. Int J Mater Prod Technol 19:362–373. https://doi.org/10.1504/IJMPT.2003.003229
3. Simončič S, Podržaj P (2014) The applicability of welding force for spot weld quality assurance. Int J Microstruct Mater Prop 9:422–432. https://doi.org/10.1504/IJMMP.2014.066921
4. Uematsu Y, Tokaji K (2009) Comparison of fatigue behaviour between resistance spot and friction stir spot welded aluminium alloy sheets. Sci Technol Weld Joi 14:62–71. https://doi.org/10.1179/136217108X338908
5. Salih OS, Ou H, Sun W, McCartney DG (2015) A review of friction stir welding of aluminum matrix composites. Mater Des 86:61–71. https://doi.org/10.1016/j.matdes.2015.07.071
6. Lacki P, Więckowski W, Wieczorek P (2015) Assessment of joints using friction stir welding and refill friction stir spot welding methods. Arch Metall Mater 60:2297–2306. https://doi.org/10.1515/amm-2015-0377
7. European Committee for Electrotechnical Standardization (CENELEC). Friction stir welding—aluminium—part 5: quality and inspection requirements. Brussels: CENELEC (2013) Standard No. EN ISO 25239-5:2013
8. American Welding Society (AWS). Specification for friction stir welding of Al alloys for aerospace applications. Miami: AWS (2009). Standard No. D17.3/D17.3M:20
9. Gibson BT, Lammlein DH, Prater TJ, Longhurst WR, Cox CD, Ballun MC, Dharmaraj KJ, Cook GE, Strauss AM (2014) Friction stir welding: process, automation, and control. J Manuf Process 16:56–73. https://doi.org/10.1016/j.jmapro.2013.04.002
10. Shen Z, Yang X, Zhang Z et al (2013) Microstructure and failure mechanisms of refill friction stir spot welded 7075-T6 aluminum alloy joints. Mater Des 44:476–486. https://doi.org/10.1016/j.matdes.2012.08.026
11. Venukumar S, Yalagi S, Muthukumaran S (2013) Comparison of microstructure and mechanical properties of conventional and refilled friction stir spot welds in AA 6061-T6 using filler plate. Trans Nonferrous Met Soc China 23:2833–2842. https://doi.org/10.1016/S1003-6326(13)62804-6
12. Rosendo T, Parra B, Tier MAD, da Silva AAM, dos Santos JF, Strohaecker TR, Alcântara NG (2011) Mechanical and microstructural investigation of friction spot welded AA6181-T4 aluminum alloy. Mater Des 32:1094–1100. https://doi.org/10.1016/j.matdes.2010.11.017
13. Campanelli LC, Suhuddin UFH, Antonialli AÍS, dos Santos JF, de Alcântara NG, Bolfarini C (2013) Metallurgy and mechanical performance of AZ31 magnesium alloy friction spot welds. J Mater Process Technol 213:515–521. https://doi.org/10.1016/j.jmatprotec.2012.11.002
14. Zhang Z, Yang X, Zhang J, Zhou G, Xu X, Zou B (2011) Effect of welding parameters on microstructure and mechanical properties of friction stir spot welded 5052 aluminum alloy. Mater Des 32:4461–4470. https://doi.org/10.1016/j.matdes.2011.03.058
15. Tran VX, Pan J, Pan T (2009) Effects of processing time on strengths and failure modes of dissimilar spot friction welds between aluminum 5754-O and 7075-T6 sheets. J Mater Process Technol 209:3724–3739. https://doi.org/10.1016/j.jmatprotec.2008.08.028
16. Merzoug M, Mazari M, Berrahal L, Imad A (2010) Parametric studies of the process of friction spot stir welding of aluminium 6060-T5 alloys. Mater Des 31:3023–3028. https://doi.org/10.1016/j.matdes.2009.12.029
17. Choi DH, Ahn BW, Lee CY, Yeon YM, Song K, Jung SB (2010) Effect of pin shapes on joint characteristics of friction stir spot welded AA5J32 sheet. Mater Trans 51:1028–1032. https://doi.org/10.2320/matertrans.M2009405
18. Xu Z, Li Z, Ji S, Zhang L (2017) Refill friction stir spot welding of 5083-O aluminium alloy. J Mater Sci Technol. https://doi.org/10.1016/j.jmst.2017.02.011

19. Zhao Y, Liu H, Yang T, Lin Z, Hu Y (2016) Study of temperature and material flow during friction spot welding of 7B04-T74 aluminium alloy. Int J Adv Manuf Technol 83:1467–1475. https://doi.org/10.1007/s00170-015-7681-2
20. Li Z, Ji S, Ma Y, Chai P, Yue Y, Gao S (2016) Fracture mechanism of refill friction stir spot-welded 2024-T4 aluminium alloy. Int J Adv Manuf Technol 86:1925–1932. https://doi.org/10.1007/s00170-015-8276-7
21. Cao JY, Wang M, Kong L, Zhao HX, Chai P (2017) Microstructure, texture and mechanical properties during refill friction stir spot welding of 6061-T6 alloy. Mater Charact 128:54–62. https://doi.org/10.1016/j.matchar.2017.03.023
22. Zhao YQ, Liu HJ, Chen SX, Lin Z, Hou JC (2014) Effects of sleeve plunge depth on microstructures and mechanical properties of friction spot welded alclad 7B04-T74 aluminium alloy. Mater Des 62:40–46. https://doi.org/10.1016/j.matdes.2014.05.012
23. Reimann M, Goebel J, Gartner TM, dos Santos JF (2017) Refilling termination hole in AA 2198-T851 by refill friction stir spot welding. J Mater Proc Technol 245:157–166. https://doi.org/10.1016/j.jmatprotec.2017.02.025
24. Reimann M, Goebel J, dos Santos JF (2017) Microstructure and mechanical properties of keyhole repair welds in AA 7075-T651 using refill friction stir spot welding. Mater Des 132:283–294. https://doi.org/10.1016/j.matdes.2017.07.013
25. American Society for Testing and Materials (ASTM). Standard practice for microetching metals and alloys. West Conshohocken: ASTM International (2007). Standard no. E407
26. Liu JT, Zhang YA, Li XW, Li ZH, Xiong BQ, Zhang JS (2014) Thermodynamic calculation of high zinc-containing Al-Zn-Mg-Cu alloy. Trans Nonferrous Met Soc China 24:1481–1487. https://doi.org/10.1016/S1003-6326(14)63216-7
27. Shen Z, Yang X, Yang S, Zhang Z, Yin Y (2016) Microstructure and mechanical properties of friction spot welded 6061-T4 aluminium alloy. Mater Des 54:766–778. https://doi.org/10.1016/j.matdes.2013.08.021
28. Mishra RS, Ma ZY (2005) Friction stir welding and processing. Mater Sci Eng R Rep 50:1–78. https://doi.org/10.1016/j.mser.2005.07.001
29. Santos TG, Miranda RM, Vilaça P, Teixeira JP, dos Santos J (2011) Microstructural mapping of friction stir welded AA 7075-T6 and AlMgSc alloys using electrical conductivity. Sci Technol Weld Joi 16:630–635. https://doi.org/10.1179/1362171811Y.0000000052
30. Baek SW, Choi DH, Lee CY, Ahn BW, Yeon YM, Song K, Jung SB (2010) Microstructure and mechanical properties of friction stir spot welded galvanized steel. Mater Trans 51:1044–1050. https://doi.org/10.2320/matertrans.M2009337
31. Dong H, Chen S, Song Y, Guo X, Zhang X, Sun Z (2016) Refilled friction stir spot welding of aluminum alloy to galvanized steel sheets. Mater Des 94:457–466. https://doi.org/10.1016/j.matdes.2016.01.066
32. Shen Z, Yang X, Yang S, Zhang Z, Yin Y (2016) Microstructure and mechanical properties of friction spot welded 6061-T4 aluminium alloy. Mater Des 54:766–778. https://doi.org/10.1016/j.matdes.2013.08.021
33. Yang XW, Fu T, Li WY (2014) Friction stir spot welding: a review on joint macro- and microstructure, property, and process modelling. Adv Mater Sci Eng, 2014, article ID 697170 doi: https://doi.org/10.1155/2014/697170
34. Zafar A, Awang M, Khan SR, Emamian S (2016) Investigating friction stir welding on thick nylon 6 plates. Weld J 95:210–218
35. Campanelli LC, Suhuddin UFH, Antonialli AIS, dos Santos JF, de Alcantara NG, Bolfarini C (2013) Metallurgy and mechanical performance of AZ31 magnesium alloy friction spot welds. J Mater Process Technol 213:515–521. https://doi.org/10.1016/j.jmatprotec.2012.11.002
36. Khan NZ, Khan ZA, Siddiquee AN, Al-Ahmari AM, Abidi MH (2017) Analysis of defects in clean fabrication process of friction stir welding. Trans Nonferrous Met Soc China 27:1507–1516. https://doi.org/10.1016/S1003-6326(17)60171-7
37. Yuan W, Mishra RS, Webb S, Chen YL, Carlson B, Herling DR, Grant GJ (2011) Effect of tool design and process parameters on properties of Al alloy 6016 friction stir spot welds. J Mater Process Technol 211:972–977. https://doi.org/10.1016/j.jmatprotec.2010.12.014
38. Pourali M, Abdollah-Zadeh A, Saeid T, Kargar F (2017) Influence of welding parameters on intermetallic compounds formation in dissimilar steel/aluminum friction stir welds. J Alloys Compd 715:1–8. https://doi.org/10.1016/j.jallcom.2017.04.272
39. Tier MD, Rosendo TS, dos Santos JF, Huber N, Mazzaferro JA, Mazzaferro CP, Strohaecker TR (2013) The influence of refill FSSW parameters on the microstructure and shear strength of 5042 aluminium welds. J Mater Process Technol 213:997–1005. https://doi.org/10.1016/j.jmatprotec.2012.12.009